# Dipole-OrientedMolecular Solids Can Undergo a Phase Change and Still Maintain Electrical Polarisation

Andrew Cassidy*[a], Mads R. V. Jørgensen, [b] Alexander Rosu-Finsen, [c] Jérôme Lasne, [c] Jakob H. Jørgensen, [a] Artur Glavic, [d, †] Valeria Lauter, [d] Bo B. Iversen, [b] Martin R.S. McCoustra, [c] and David Field.[a]

[a] A Cassidy*, JH Jørgensen, D. Field, Department of Physics and Astronomy, Aarhus University, Ny Munkegade 120, Aarhus C, Denmark. E-mail: amc@phys.au.dk. Telephone: +45 87155584.

[b] MRV Jørgensen, BB Iversen, Center of Materials Crystallography, iNano & Department of Chemistry, Aarhus University, Langelandsgade 140, Aarhus C, Denmark

[c] A Rosu-Finsen, J. Lasne, MRS McCoustra, Institute of Chemical Sciences, Heriot-Watt University, Riccarton, EH14 4AS Edinburgh, United Kingdom

[d] A Glavic†, V Lauter, Quantum Condensed Matter Division, Oak Ridge National Lab, Oak Ridge, TN 37831, USA.

*Corresponding Author

† Present Address Artur Glavic, Laboratory for Neutron Scattering and Imaging, Paul Scherrer Institut, 5232 Villigen PSI, Switzerland.

## Author Contributions

The manuscript was written through contributions of all authors.

**Abstract**

It has recently been demonstrated that nanoscale molecular films can spontaneously assemble to self-generate intrinsic electric fields that can exceed $10^8$ V/m. These electric fields originate from polarisation charges in the material which arise because the films self-assemble to orient molecular dipole moments. This has been called the spontelectric effect. Such growth of spontaneously polarized layers of molecular solids has implications for our understanding of how intermolecular interactions dictate the structure of molecular materials used in a range of applications, for example, molecular semiconductors, sensors, and catalysis. Here we present the first in situ structural characterisation of a representative spontelectric solid, nitrous oxide. Infrared spectroscopy, temperature programmed desorption and neutron reflectivity measurements demonstrate that polarised films of nitrous oxide undergo a structural phase transformation upon heating above 48 K. A meanfield model can be used to quantitatively describe the magnitude of the spontaneously generated field as a function of film-growth temperature and this model also recreates the phase change. This reinforces the spontelectric model as a means of describing long range dipole-dipole interactions and points to a new type of ordering in molecular thin films.

## Introduction

Understanding the processes that govern the nucleation of metastable phases of molecular solids remains a challenge and requires a microscopic approach to molecular interactions in the search for solutions.[1–3] Single-phase molecular solids are increasingly cherished for their opto-electronic properties and find use as sensors, semiconductors and mechanical actuators; molecular solids are often cheaper, lighter and safer than their inorganic counterparts.[4–8] Predicting the phase structure of molecular solids is complicated by the myriad of interactions which can exist between the constituent species. Recently, a new class of spontaneously polarised molecular solids has been proposed where the phase structure of the entire film is governed chiefly by long range dipole-dipole interactions.

The “spontelectric effect” describes the spontaneous evolution of electric fields in molecular solids, up to $10^8$ V/m, resulting from the self-assembly of molecular dipoles *en masse* throughout thin films grown by physical vapour deposition (PVD).[9–16] These fields manifest as voltages that increase linearly with film thickness, measured at the film-vacuum interface relative to the back side of the film. The generated electric fields have also been shown to produce a Stark shift in vibrational modes with a component along the field axis.[16] This effect has been successfully modelled by invoking long-range ordering of molecular dipoles throughout the solid, giving rise to macroscopic polarisation which produces the observed voltages. The spontaneous nature in which molecules polarise upon film growth to produce these electric fields in combination with the man-

ner in which the field strength changes as the film deposition temperature varies, distinguishes this polarised state from other polarised states of molecular solids.

For a spontelectric solid in the steady state, the degree of polarisation observed is strongly correlated to the temperature of film growth, with less polarisation when the deposition temperature is increased, although this is contradicted by the behaviour of methyl formate, see ref.[12] Once formed, however, the degree of polarisation in the film remains fixed in response to annealing until some critical temperature is reached, termed the Curie temperature by analogy with ferromagnetism, above which the static electric field dissipates.[11]

A mean field model was constructed to describe the observed electric field values and to quantify the interactions which give rise to the deposition temperature dependence of the spontelectric effect.[9,11,12] This model is described in detail elsewhere but is summarized here to guide the ensuing discussion.[9] In the model, the mean field experienced by any individual molecular dipole can be divided between a conventional symmetric field, $\langle E_{sym} \rangle$, which originates from intermolecular interactions on the local, microscopic scale and an asymmetric field, $\langle E_{asym} \rangle$, which arises spontaneously through macroscopic dipole orientation. These two fields combine to produce the electric field experienced by individual molecular dipoles. In the z-direction, normal to the substrate, $E_z$ is the field experienced by any given dipole. A term, $\langle E_{sym} \rangle \zeta (\langle \mu_z \rangle / \mu)^2$, acts to limit dipole rotation in the solid, Eq. 2.

$$E_z = \langle E_{sym} \rangle (1 + \zeta (\langle \mu_z \rangle / \mu)^2 ) - \langle E_{asym} \rangle (\langle \mu_z \rangle / \mu) \qquad (2)$$

where $\mu_z$ represents the z-component of the molecular dipole and $\langle\mu_z\rangle/\mu$ defines the fraction of molecular dipole oriented along the surface normal. Dipole-dipole related interactions between molecules, which depend on $(\langle\mu_z\rangle/\mu)^2$, are summed under the umbrella term of $\langle E_{sym}\rangle$ and there is no residual $\langle E_{sym}\rangle$ in any direction within the film. The observed electric field, $E_{obs}$, oriented normal to the surface plane, is given by $\langle E_{asym}\rangle\langle\mu_z\rangle/\mu$. The film self-generates $\langle E_{asym}\rangle\langle\mu_z\rangle/\mu$ *via* a non-linear, non-local feedback process; dipole orientation in the direction normal to the substrate gives rise to an asymmetric field and once this field originates, dipoles are preferentially oriented with regard to its influence. The defining characteristic of a spontelectric solid is that the intrinsic static electric field arises spontaneously upon film growth and that this "spontelectric field" maintains dipole orientation against competing thermal mechanisms which act to disorient the molecular dipoles. In this way the spontelectric field is analogous to the Weiss field in ferromagnetic solids. There is no equivalent description of ordering forces in contemporary descriptions of molecular solids.

The ordering of dipoles is tempered by thermal motion and as such is governed by the Langevin equation, Eq. 3

$$\langle\mu_z\rangle/\mu = \coth(E_z\,\mu / T) - (E_z\,\mu / T)^{-1} \qquad (3)$$

where T is the temperature of the film deposition expressed in atomic units. The molecular dipole moment is altered from the gas phase dipole moment, $\mu_0$, by the presence of surrounding molecular dipoles in the condensed phase such that

$$\mu = \mu_0 / (1 + \alpha k / s^3) \quad (4)$$

where α is the molecular polarizability (22.23 au for nitrous oxide), k (=11.034) is a constant dictated by the structural relationship between dipoles in a lattice arrangement and s is the interlayer spacing.[17] The spontelectric model is parameterised, and up to the present, $<E_{sym}>$, ζ and s have acted as variables to produce fits to experimental values of $E_{obs}$.[11–15]

Up to now it has been assumed that $<E_{sym}>$, ζ and s act as temperature independent variables and can be used to describe the spontelectric phase structure of a film across a broad temperature range. Here we present the first structural characterization, as a function of film temperature, of a spontelectric material, using thin films of nitrous oxide as a representative member of the spontelectric class.[11] Our objective is to test the assumption that the spontelecstric parameters can be taken as temperature independent or whether the structural-phase behavior of spontelectric films has an influence on the polarization properties.

**Experimental**

Neutron reflectivity data was collected at the Magnetism Reflectometer instrument at the Spallation Neutron Source at Oak Ridge National Laboratory.[18] A silica substrate was mounted on a closed cycle helium cryostat allowing for cooling down to 20 K under high vacuum conditions with a base pressure of approximately $1\times10^{-7}$ mbar. Nitrous oxide (99.998 %) was deposited from a gas line with a base pressure below $1\times10^{-6}$ mbar.

A standard needle valve was used to expose a silica substrate to a controlled background pressure of nitrous oxide, with a substrate temperature of 38 K to avoid $N_2$ adsorption. The rate of deposition was 5 Å/min. A highly collimated neutron beam was incident on the sample under a grazing angle Θ and the scattered neutrons were registered by a 2D neutron detector as a function of time-of-flight and scattering angle. Choppers constrain the total bandwidth of the neutron beam incident on the sample to ~3 Å when operating at 60 Hz. The experiments were performed with neutron wavelength bands of 2.9 to 5.9 Å and 5.1 to 8.1 Å. The time-of-flight directly correlates to the neutron wavelength, λ, and thus the momentum transfer perpendicular to the sample surface can be calculated using

$$Q_z = 4\pi\sin\Theta/\lambda \qquad (1)$$

Neutron reflectometry probes the depth profile of the scattering length density (SLD) of the film, the product of molecular density and neutron scattering length. The depth resolution of the Magnetism Reflectometer is defined by the Q-range which here gives 0.5 nm. For each reflectivity 5 measurements were performed using different wavelength bands and Θ angles to cover a $Q_z$ range from <0.01 $Å^{-1}$ to 0.16 $Å^{-1}$ with 2% relative resolution $\Delta Q_z/Q_z$. Reflectivities were collected repeatedly from a thick nitrous oxide sample over a 3 hour period to check the stability of the measuring conditions.

Modelling of the NR data was performed using the standard Paratt recursion formalism[19] implemented in the GenX software.[20] The substrate part of the model was first refined with a measurement before film growth and later kept constant. The nitrous oxide film data could not be refined with a single, homogeneous layer so the film SLD depth profile was built from several sublayers with varying denstities. To keep the model

physically reasonable the layer parameters were constrained to values that did not allow an increase of the density at larger distance from the substrate. This is justified on the basis that voids should not form within a deposited layer.

Reflection-absorption infrared spectroscopy (RAIRS) and temperature programmed desorption (TPD) data were collected in a UHV chamber (base pressure of $2\times10^{-10}$ mbar) equipped with a quadrupole mass spectrometer (QMS, Hiden Analytical Ltd, HAL301), an IR spectrometer (Varian 670-IR) and a Cu substrate cooled with a closed-cycle He cryostat (base temperature of 20 K).[21,22] Silica layers were prepared on the Cu substrate in vacuum as required. The temperature of molecular films, grown in dark conditions by background vapour deposition, was controlled with a cartridge heater (Heatwave Labs, Inc.) located inside the Cu sample block and monitored with a KP-thermocouple in connection with an IJ-6 temperature controller (IJ Instruments). For RAIRS experiments a non-polarised IR beam at a grazing incidence of 75° was reflected off the sample and detected with a liquid nitrogen cooled mercury cadmium-telluride detector. A total of 512 scans were taken per spectrum with a resolution of 1 $cm^{-1}$. For the TPD experiments, separate molecular mixtures of $N_2O$ with $O_2$ and $N_2$ were prepared in the dosing lines prior to deposition; a heating rate of 0.1 K/s was used and desorption was detected with the mass spectrometer.

Surface potential measurements were performed in a UHV chamber (base pressure of $2\times10^{-10}$ mbar) attached to the SGM2 beamline at the ASTRID synchrotron storage ring at Aarhus University. Films of nitrous oxide were prepared by background dosing techniques, on a polycrystalline gold substrate cooled with a closed-cycle He cryostat. Note that there is no substrate effect on the magnitude of the spontelectric effect.[14] The sur-

face of a film was irradiated with a collimated beam of 5 meV electrons (±1.5 meV) produced by threshold photoionization of Ar. The sample was floated, relative to ground, until the onset of current flow (2-3 fAmp) was detected by an ammeter connected to the backside of the film. The bias used to float the sample was exactly opposite in value to the potential residing at the film-vacuum interface.[9]

Comparisons are made between the properties of nitrous oxide films prepared in three different experimental set ups, each equipped with a closed cycle He cryostat. In each case the temperatures reported were calibrated to be as accurate as possible. Temperature sensitive diodes, mounted on the cryostat cold finger, were used for these calibrations and K-type thermocouples, mounted close to the substrate, were used to measure the temperatures reported here. We report that nitrous oxide undergoes a phase transition when heated above 48 K, but allow for systematic errors of ±1 K in temperature measurements between different experimental set ups.

**Results**

First we use structural characterization techniques namely neutron reflectivity data, reflection-absorption infrared spectroscopy data and temperature programmed desorption data to show that thin films of nitrous oxide undergo a phase change when heated above 48 K. Then we relate this phase change to the electronic properties of spontaneously polarized films of nitrous oxide by fitting electrical measurements of self-generated internal electric fields with the spontelectric model.

Neutron reflectivity data sets, Figure 1a, were recorded on the primary film, grown at 38 K and again after this film was annealed to progressively higher temperatures. Films

were cooled to 20 K after each annealing step for data collection. The experimental data sets, black points in Figure 1a, for the primary film and films annealed up to 44 K are identical and overlap in Figure 1a. These data relate to a low temperature phase and other data (not shown here) confirm the stability of films at these temperatures over the relevant time scales. Data for films annealed to 47 K and above show changes in the reflectivity profiles and we relate this to the evolution of a high temperature phase. The results of fits, constructed following the procedure described in the experimental section, are presented as solid lines in Figure 1a. The corresponding scattering length density (SLD) profiles obtained from the fits to the data for each annealing temperature are shown in Figure 1b. The SLD profiles for films of nitrous oxide have been converted to density depth profiles, right hand-axis in Figure 1b, by multiplying with the nitrous oxide mass density per scattering length ($2.979 \times 10^{5}$ (g.Å$^{2}$).cm$^{-3}$).

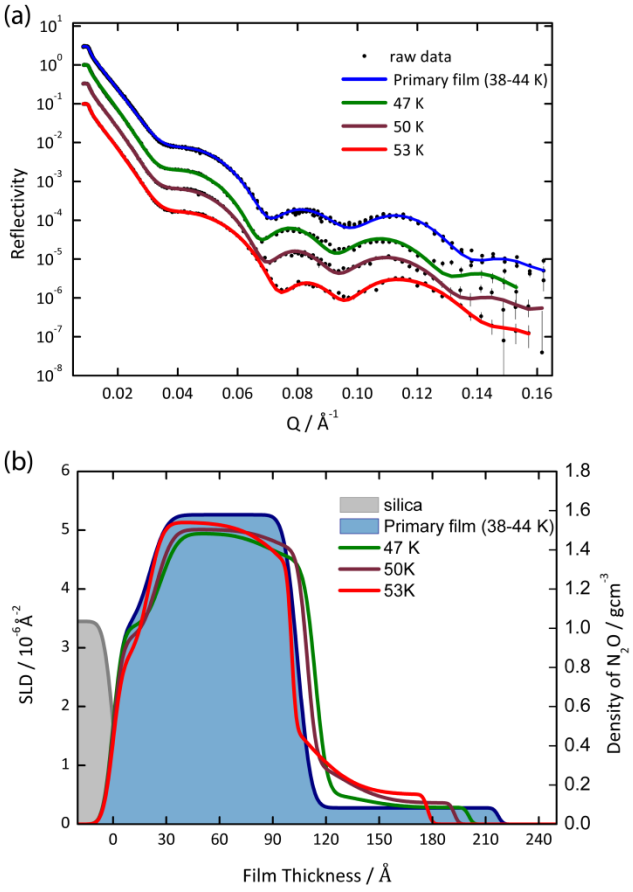


Figure 1. Neutron reflectometry results for in-situ grown nitrous oxide films. a) Neutron reflectivity data from a film heated from 38 K (navy - top) to 53 K (red - bottom). Fits to the experimental data sets are shown as solid lines. All of the experimental data between 38 K and 44 K overlap and can be fit with the same model, represented by the “Primary” curve. Curves are offset on the y-axis for clarity. b) The scattering length density depth profiles obtained from the fits to the data in a) are presented as a function of film thickness, for films annealed to progressively higher temperatures. The axis on the right hand side corresponds to the density of the nitrous oxide film.

The density profiles in Figure 1b are presented as a function of the nitrous oxide film thickness with 0 Å marking the interface between the silica substrate and molecular film. The interface between the silica substrate and the nitrous oxide film is rather ab-

rupt, extends over <10 Á and represents the roughness of the silica substrate, in concurrence with reflectivity data from the clean silica substrate. Once the nitrous oxide film has grown thicker than the rough layer on the silica substrate the density of the molecular layer reaches its bulk value. For the low temperature phase (38-44 K marked primary film in Figure 1b), the film is approx. 100 Å thick and has a density of 1.57 g $cm^{-3}$. This density remains constant throughout the film. We attribute the extended very low density profile from 120 Å onwards to the adsorption of impurities (nitrogen, oxygen and water) on the surface of the nitrous oxide film when cooled to 20 K for measurements. We will later show that nitrogen and oxygen condense at temperatures below 35 K (Figure 3) and separate NR measurements (not shown here) confirm that nitrogen and oxygen co-condense with nitrous oxide when films are grown below these temperatures. We therefore expect that the nitrous oxide film grown at 37 K is pure and did not contain nitrogen or oxygen contaminants but that by cooling the film to 20 K for measurements some nitrogen and oxygen impurities are likely to have condensed at the film-vacuum interface. The effect of dosing either polarized or unpolarised layers on top of spontelectric films has previously been considered was demonatrated not to affect the electric field stored in the underlying spontelectric layer.[14] Hence we do not expect any contribution from these impurities towards charge screening process that may influence the phase structure of the nitrous oxide layer.

Once heated to 47 K the density of the film drops to 1.47 g $cm^{-3}$ and the film thickness increases by 15 Å. At 50 K the density partially recovers to 1.51 g $cm^{-3}$ and at 53 K the film thickness moves back to 100 Å. In the high temperature phase (47-53 K) the densi-

ty depth profile is no longer constant over the entire film and the film-vacuum interface becomes more diffuse, with a less-sharp boundary.

Assuming that the FCC cubic lattice structure of nitrous oxide persists over the entire temperature range (38-53 K) then the density of the primary nitrous oxide film gives a unit cell length of 5.71 Å.[23] This corresponds well with the unit cell length of 5.67 Å, reported from earlier neutron diffraction measurements on macroscopic crystals of nitrous oxide.[23] For convenience we choose the density at 51 K to represent the high temperature phase giving a unit cell length of 5.81 Å. As the unit cell is FCC, we assume two layers of nitrous oxide per unit cell, giving $s_L$ = 2.855 Å and $s_H$ = 2.905 Å, where subscripts L and H refer to the low temperature (<47 K) and high temperature (> 47 K) phases respectively. These values may be compared with that of 3.2 Å obtained from fitting electric field measurements.[11]

Turning now to RAIRS data we note that when molecules condense to form a solid, collective vibrations of molecular bonds can extended throughout the solid to form phonons. These phonons can couple to, and split, fundamental vibrational frequencies. In Figure 2 reflection-absorption infrared spectroscopy (RAIRS) data show a step change in the absolute and relative frequencies of the longitudinal optical (LO) and transverse optical (TO) phonon peaks of the vNN vibrational mode in films of nitrous oxide annealed to above 48 K. Films were grown at 20 K on a silica substrate and heated to progressively higher temperatures, with cooling to 20 K after each annealing step for data collection. Longitudinal phonons resonate at higher frequencies because of the induced field associated with longitudinal waves passing through a dipolar medium. The presence of LO and TO phonon modes in all spectra, though extensively inhomogene-

ously broadened at lower temperatures, suggests collective oscillations throughout the solid. This implies that the phase nucleated at 20 K exhibits ordering behaviour. By growing the molecular layer on a clean Cu substrate metal surface selection rules dictate that the TO vibrations remain silent.[24] Thus the TO phonon mode is eliminated and only the LO phonon peak survives, as shown in the lower plot, offset on the y-axis, in Figure 2. The LO peak for a film deposited at 20 K on a Cu substrate, Figure 2, can be fitted with a Gaussian peak, with a full width at half maximum (FWHM) of 6 $cm^{-1}$, and frequency, $\omega(LO_{20})$ = 2252 $cm^{-1}$. This may be compared with the FWHM of 2 $cm^{-1}$ used to fit the LO peak at $\omega(LO_{50})$ = 2257 $cm^{-1}$ after annealing above 48 K. The broad TO peak centred at 2225 $cm^{-1}$ for films grown at 20 K on silica narrows and shifts to 2239 $cm^{-1}$ upon annealing above 48 K. Similar results (not shown here) have been obtained for films deposited, as opposed to annealed, across the same temperature range (from 20-52 K).

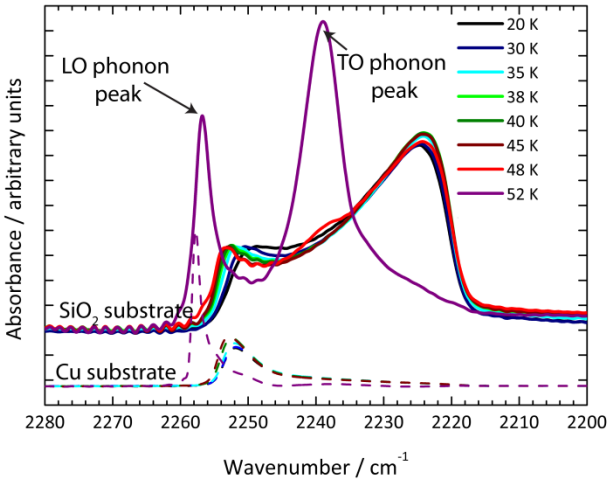


Figure 2. RAIRS data for a film of nitrous oxide deposited at 20 K on a silica substrate and subsequently annealed to progressively higher temperatures. All spectra were recorded at 20 K. Only data for the

vNN peak are shown. Data for a film of nitrous oxide deposited on a Cu substrate are offset on the y-axis for clarity. Only the LO mode is visible on the clean metal substrate.

The extent of LO-TO splitting is largely determined by the spacing between molecular dipoles in a unit cell.[25] We relate the abrupt change in the positions and shapes of phonon peaks to a phase change in the material. The reduction in the LO-TO splitting suggests an increase in molecular spacing on moving from the low temperature phase to the high temperature phase, in agreement with density profile measurements obtained from NR experiments. In the low temperature phase there is strong absorption between the LO and TO peaks, emphasised at 2240 $cm^{-1}$ where a small feature begins to emerge at 48 K. In addition the broad peaks representing the LO and TO phonons in the lower temperature spectra suggest a poorly defined unit cell in the low temperature phase. The low temperature film is heavily positionally disordered.[26] Neutron diffraction experiments would confirm any crystallinity and were attempted but the intensity of scattering from the film was too low to obtain a diffraction pattern in the time available.

Temperature programmed desorption (TPD) data corresponding to films composed of mixtures of $N_2$, $O_2$ and $N_2O$ grown under UHV ($1\times10^{-10}$ mbar) on silica at 20 K are shown in Figure 3. Data for $N_2O$, (black curve) show complete desorption represented by a single peak at 80 K. Data for $O_2$ (red) and $N_2$ (blue) show: i) Broad, low temperature peaks with a maximum at 31 K (35 K) corresponding to desorption of $O_2$ ($N_2$) physisorbed on top of the composite film.[27] ii) Peaks with leading edges starting at 48 K resolving to peaks at 51 K are attributed to $O_2$ and $N_2$ released from the $N_2O$ matrix upon a structural rearrangement within the $N_2O$ film. Such features are termed volcano

peaks.[28] 48 K corresponds very well with the temperature for the phase change inferred to occur from our interpretation of the NR data in Figure 1, and RAIRS data in Figure 2. iii) Peaks between 55-70 K are related to desorption from the cold finger and sample mount and are not relevant to the discussion, and iv) species released at 80 K when the $N_2O$ film itself desorbs.

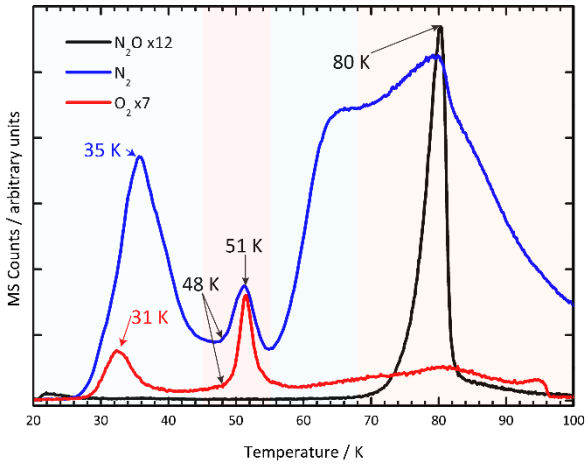


Figure 3.Temperature programmed desorption data for masses 44 amu ($N_2O$ black trace), 32 amu ($O_2$ red trace) and 28 amu ($N_2$ blue trace).

Having demonstrated that thin films of nitrous oxide undergo a phase change when heated above 48 K we now move to examine the behaviour of molecular dipole alignment in reponse to this phase change.

The evolution of surface voltages, as a function of film thickness in monolayers (ML), and film deposition temperature, have previously been reported for thin films of nitrous oxide and are shown in the inset in Figure 4a.[10,11] At any given film deposition temperature, surface voltage increases linearly with film thickness. Given the layer spacing, ta-

ble 1, the slope of each line in the inset gives the static electric field harboured by the film at that growth temperature. This is plotted as black squares in Figure 4a. Field strength drops with deposition temperature. This is in contrast to the almost constant magnitude of the field in films deposited at a low temperature and then annealed close to desorption temperature (Figure 4b).

**Table 1. The parameters used to create the new fits to the experimental surface potential measurements shown in Fig 4.**

| Low Temp phase < 48 K | High Temp phase > 48 K |
|---|---|
| $s_{L^*}$ = 2.855 Å | $s_H$ = 2.905 Å |
| $\langle E_{sym} \rangle_L = 7.79 \times 10^8$ V/m | $\langle E_{sym} \rangle_H = 6.01 \times 10^8$ V/m |
| $\langle E_{asym} \rangle_L = 6.69 \times 10^8$ V/m | $\langle E_{asym} \rangle_H = 6.92 \times 10^8$ V/m |
| $\zeta_L$ = 26.8 | $\zeta_H$ = 57.5 |

* Parameters for the low temperature and high temperature phases of the nitrous oxide film are delineated by the subscripts L and H respectively.

Using the values of $s_L$ and $s_H$ from NR measurements the spontelectric model can be used to fit the data, as shown in Figure 4a. To do so, it is necessary to change the values of $\langle E_{sym} \rangle$ and $\zeta$ at 48 K. No one parameter set produces a satisfactory fit to all of the data across the temperature range 38-65 K.

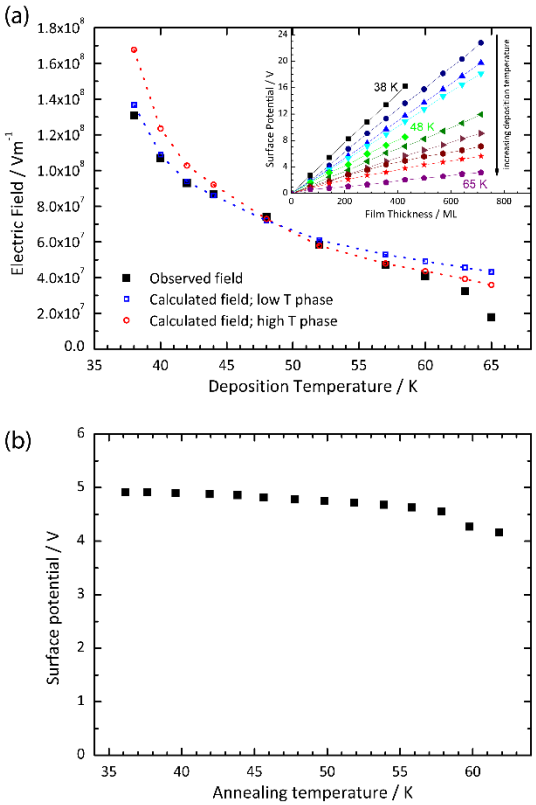


Figure 4. a) The electric field measured in films of $N_2O$ plotted as a function of film deposition temperature (black squares), with the calculated fields for the low temperature (blue squared) and high temperature phase (red circles) superimposed. The lines act as a guide to the eye. The inset shows how surface potentials develop as a function of film thickness across a range of film deposition temperatures (38-65 K). b) Surface potential of a film of $N_2O$ deposited at 38 K and annealed in steps up to 62 K. At each temperature time was given to reach thermal equilibrium and then the surface potential at the film-vacuum interface was measured.

The parameters used to produce the fits to $E_{obs}$ are listed in Table 1. Only $\langle E_{sym} \rangle$ and $\zeta$ are free parameters in constructing the fit. As the deposition temperature increases above 60 K the calculated and observed fields begin to diverge. The TPD data in Figure 3 give a leading edge for film desorption, upon annealing, at 68 K and it is consistent to assume that deposition at temperatures close to 68 K does not lead to a steady state

film. The mean field model is therefore no longer appropriate because of large fluctuating motions in the medium.

## Discussion

Previous results have shown that PVD grown films of nitrous oxide, deposited between 38-65 K, spontaneously polarise upon growth and harbour static electric fields.[11] Here we have shown, through RAIRS, TPD and NR data, that this temperature range gives access to two distinct structural phases of nitrous oxide. RAIRS data suggest an increase in the size of the unit cell on annealing above 48 K and NR measurements confirm a decrease in film density at the same temperature. The dynamics of this unit cell expansion facilitate the release of trapped gases in the TPD experiments and give rise to the volcano peaks for $O_2$ and $N_2$, also at 48 K (Figure 3).[28] The spontelectric model accurately quantifies the drop in the spontelectric field in films deposited between 38 K and 44 K. This drop in field with increasing deposition temperature arises from thermally induced disorder in dipole alignment. Thermally induced disorder alone, however, is not sufficient to explain the drop in fields above 48 K and the changes introduced into the spontelectric model above this temperature reflect the structural changes detected in the film by RAIRS and NR data. The increase in dipole separation, and the corresponding increase in layer spacing, forced by annealing above 48 K is reflected by the observed decrease in the value of $\langle E_{sym} \rangle$ moving from the low to the high temperature phase (table 1). As the unit cell expands and dipoles move apart, $\langle E_{sym} \rangle$ is expected to decrease since intermolecular interactions are weaker. RAIRS and NR data were collected from films grown at low temperature and then annealed, while the spon-

telectric model has been applied to films grown at different temperatures. The structural phase change occurs regardless as to how the sample is prepared while the spontelectric phase change only occurs if films are deposited at low or high temperatures. If a film is deposited at 38 K and annealed to 52 K the surface potential drops by only 4%, meaning that the polarisation inherent in the film survives the structural phase change. Annealing of films grown in the low temperature phase does not lead to a significant drop in the spontelectric field as the annealing temperature crosses the phase boundary (Figure 4b). By contrast the difference in surface potential for films of the same thickness individually deposited at 38 K or 52 K is >50%.

The expansion of the unit cell on moving from the low temperature to the high temperature phases is accompanied by a 23% decrease in $\langle E_{sym} \rangle$, but $\langle E_{asym} \rangle$ increases by only 3% over the same temperature range. The implication is that the value of $\langle E_{asym} \rangle$ appears to be intrinsic to the molecular constituents, while the value of $\langle E_{sym} \rangle$ appears to vary as a function of the environment in which the molecular constituents find themselves. This phenomenon was also evinced and discussed in relation to the dilution of nitrous oxide in xenon matrices.[15] Increasing the degree of dilution, akin to moving the nitrous oxide molecules further apart, led to a reduction in $\langle E_{sym} \rangle$, while the value of $\langle E_{asym} \rangle$ remained almost constant at all dilutions, until a threshold dilution was reached above which the spontelectric field failed to establish.

## Conclusion

The potential energy landscape of solids contains many metastable habitable zones. We have demonstrated that the spontelectric model, in which polarization arises from

molecular dipole orientation, can be used to describe a dipole-ordered phase for molecular films. The inclusion in the spontelectric model of long range, non-local interactions between molecular dipoles and the spontaneously generated static electric field is essential in order to fit the observed experimental results. Such non-local, non-linear interactions are not currently included in other models describing phases of molecular solids and these results further secure the spontelectric model in describing a new class of molecular solids.

We note that the presence of a polarization field implies non-linear optical properties.[29] Experimental methodologies for the growth and characterisation of functional films of molecular solids are attracting attention in the search for opto-electrically active materials.[8,30–33] The system considered here requires cryogenic temperatures and high-vacuum conditions, but offers a fertile environment for fundamental studies considering non-covalent intermolecular interactions. To move spontelectrics toward applications, efforts are required to find molecular materials which remain spontaneously polarised at higher temperatures. To date toluene, which remains polarised at 90 K, leads the charge.[11]

**Acknowledgement**

We gratefully acknowledge support of the staff of the Aarhus Synchrotron Radiation Laboratory (ISA), the Danish Research Council, DANSCATT, European Community FP7-ITN Marie-Curie Programme (LASSIE project, grant agreement #238258) (AC, JL), Heriot-Watt University for a James Watt scholarship (ARF) and the Danish National Research Foundation (DNRF93) (MRVJ, BBI). The research performed at ORNL's Spallation Neutron Source was sponsored by the Scientific User Facilities Division, Office of

Basic Energy Sciences, US Department of Energy. We higly appreciate the support of H. Ambaye and R. Goyette during the preparation of the equipment for the NR experiments.

**References**

(1) Guo, X.; Liao, Q.; Manley, E. F.; Wu, Z.; Wng, Y.; Wang, W.; Yang, T.; Young-Eun, S.; Cheng, X.; Liang, Y.; et al. Materials Design via Optimized Intramolecular Non-Covalent Interactions for High-Performance Organic Semiconductors. *Chem. Mater.* **2016**, *28*, 2449–2460.

(2) Chen, S.; Enders, A.; Zeng, X. C. Influence of Structural Fluctuations, Proton Transfer, and Electric Field on Polarization Switching of Supported Two-Dimensional Hydrogen-Bonded Oxocarbon Monolayers. *Chem. Mater.* **2015**, *27* (13), 4839–4847.

(3) Davey, R. J.; Schroeder, S. L. M.; Ter Horst, J. H. Nucleation of Organic Crystals - A Molecular Perspective. *Angew. Chemie - Int. Ed.* **2013**, *52* (8), 2167–2179.

(4) Horiuchi, S.; Tokura, Y. Organic Ferroelectrics. *Nat Mater* **2008**, *7* (5), 357–366.

(5) Desiraju, G. R. Crystal Engineering: A Holistic View. *Angew. Chem. Int. Ed. Engl.* **2007**, *46* (44), 8342–8356.

(6) Martins, P.; Lanceros-Méndez, S. Polymer-Based Magnetoelectric Materials. *Adv. Funct. Mater.* **2013**, *23* (27), 3371–3385.

(7) Mas-Torrent, M.; Rovira, C. Role of Molecular Order and Solid-State Structure in Organic Field-Effect Transistors. *Chem. Rev.* **2011**, *111* (8), 4833–4856.

(8) Fu, D.-W.; Cai, H.-L.; Liu, Y.; Ye, Q.; Zhang, W.; Zhang, Y.; Chen, X.-Y.; Giovannetti, G.; Capone, M.; Li, J.; et al. Diisopropylammonium Bromide Is a

High-Temperature Molecular Ferroelectric Crystal. *Science* **2013**, *339* (6118), 425–428.

(9) Field, D.; Plekan, O.; Cassidy, A.; Balog, R.; Jones, N. C.; Dunger, J. Spontaneous Electric Fields in Solid Films: Spontelectrics. *Int. Rev. Phys. Chem.* **2013**, *32* (3), 345–392.

(10) Balog, R.; Cicman, P.; Jones, N.; Field, D. Spontaneous Dipole Alignment in Films of N2O. *Phys. Rev. Lett.* **2009**, *102* (7), 2–5.

(11) Plekan, O.; Cassidy, A.; Balog, R.; Jones, N. C.; Field, D. A New Form of Spontaneously Polarized Material. *Phys. Chem. Chem. Phys.* **2011**, *13* (47), 21035–21044.

(12) Plekan, O.; Cassidy, A.; Balog, R.; Jones, N. C.; Field, D. Spontaneous Electric Fields in Films of Cis-Methyl Formate. *Phys. Chem. Chem. Phys.* **2012**, *14* (28), 9972–9976.

(13) Cassidy, A.; Plekan, O.; Balog, R.; Jones, N. C.; Field, D. Spontaneous Electric Fields in Films of CF(3)Cl, CF(2)Cl(2) and CFCl(3). *Phys. Chem. Chem. Phys.* **2012**, *15*, 108–113.

(14) Cassidy, A.; Plekan, O.; Balog, R.; Dunger, J.; Field, D.; Jones, N. C. Electric Field Structures in Thin Films: Formation and Properties. *J. Phys. Chem. A* **2014**, *118* (33), 6615–6621.

(15) Cassidy, A.; Plekan, O.; Dunger, J.; Balog, R.; Jones, N. C.; Lasne, J.; Rosu-Finsen, A.; McCoustra, M. R. S.; Field, D. Investigations into the Nature of Spontelectrics: Nitrous Oxide Diluted in Xenon. *Phys. Chem. Chem. Phys.* **2014**, *16* (43), 23843–23853.

(16) Lasne, J.; Rosu-Finsen, A.; Cassidy, A.; McCoustra, M. R. S.; Field, D. Spontaneously Electrical Solids in a New Light. *Phys. Chem. Chem. Phys.* **2015**, *17* (32), 20971–20980.

(17) Topping, J. On the Mutual Potential Energy of a Plane Network of Doublets. *Proc. R. Soc. Lond. A. Math. Phys. Sci.* **1927**, *114*, 67–72.

(18) Lauter, V.; Ambaye, H.; Goyette, R.; Hal Lee, W. T.; Parizzi, A. Highlights from the Magnetism Reflectometer at the SNS. *Phys. B* **2009**, *404* (17), 2543–2546.

(19) Parratt, L. G. Surface Studies of Solids by Total Reflection of X-Rays. *Phys. Rev.* **1954**, *95* (2), 359–369.

(20) Björck, M.; Andersson, G. GenX: An Extensible X-Ray Reflectivity Refinement Program Utilizing Differential Evolution. *J. Appl. Crystallogr.* **2007**, *40* (6), 1174–1178.

(21) Fraser, H. J.; Collings, M. P.; McCoustra, M. R. S. Laboratory Surface Astrophysics Experiment. *Rev. Sci. Instrum.* **2002**, *73* (5), 2161.

(22) Frankland, V. L.; Rosu-Finsen, a.; Lasne, J.; Collings, M. P.; McCoustra, M. R. S. Laboratory Surface Astrochemistry Experiments. *Rev. Sci. Instrum.* **2015**, *86* (5), 055103.

(23) Hamilton, W. C.; Petrie, M. Confirmation of Disorder in Solid Nitrous Oxide by Neutron Diffraction. *J. Phys. Chem.* **1961**, *65* (c), 1453.

(24) Palumbo, M. E.; Baratta, G. a; Collings, M. P.; McCoustra, M. R. S. The Profile of the 2140 Cm(-1) Solid CO Band on Different Substrates. *Phys. Chem. Chem. Phys.* **2006**, *8* (2), 279–284.

(25) Sherwood, P. M. A. *Vibrational Spectroscopy of Solids*; Cambridge Univeristy

Press: Cambridge, UK, 1972.

(26) Ovchinnikov, M. A.; Wight, C. A. Inhomogeneous Broadening of Infrared and Raman Spectral Bands of Amorphous and Polycrystalline Thin Films. *J. Chem. Phys.* **1993**, *99* (5), 3374.

(27) Collings, M. P.; Frankland, V. L.; Lasne, J.; Marchione, D.; Rosu-Finsen, A.; McCoustra, M. R. S. Probing Model Interstellar Grain Surfaces with Small Molecules. *Mon. Not. R. Astron. Soc.* **2015**, *449* (November), 1826–1833.

(28) Smith, R.; Huang, C.; Wong, E.; Kay, B. The Molecular Volcano: Abrupt CCl4 Desorption Driven by the Crystallization of Amorphous Solid Water. *Phys. Rev. Lett.* **1997**, *79* (5), 909–912.

(29) Ito, E.; Washizu, Y.; Hayashi, N.; Ishii, H.; Matsuie, N.; Tsuboi, K.; Ouchi, Y.; Harima, Y.; Yamashita, K.; Seki, K. Spontaneous Buildup of Giant Surface Potential by Vacuum Deposition of Alq[3] and Its Removal by Visible Light Irradiation. *J. Appl. Phys.* **2002**, *92* (12), 7306–7310.

(30) Ramesh, R.; Spaldin, N. A. Multiferroics: Progress and Prospects in Thin Films. *Nat. Mater.* **2007**, *6* (1), 21–29.

(31) Nguyen, T. D.; Mao, S.; Yeh, Y.-W.; Purohit, P. K.; McAlpine, M. C. Nanoscale Flexoelectricity. *Adv. Mater.* **2013**, *25* (7), 946–974.

(32) Xu, B.; Luo, Z.; Gao, W.; Wilson, A. J.; He, C.; Chen, X.; Yuan, G.; Dai, H.-L.; Rao, Y.; Willets, K.; et al. Solution-Processed Molecular Opto-Ferroic Crystals. *Chem. Mater.* **2016**, *28* (7), 2441–2448.

(33) Polyakov, A. O.; Arkenbout, A. H.; Baas, J.; Blake, G. R.; Meetsma, A.; Caretta, A.; Van Loosdrecht, P. H. M.; Palstra, T. T. M. Coexisting Ferromagnetic and

Ferroelectric Order in a CuCl4-Based Organic-Inorganic Hybrid. *Chem. Mater.* **2012**, *24* (1), 133–139.